© 2005 Nature Publishing Group http://www.nature.com/naturemethods

Optical sectioning microscopy

José-Angel Conchello[1,2] & Jeff W Lichtman[3]

Confocal scanning microscopy, a form of optical sectioning microscopy, has radically transformed optical imaging in biology. These devices provide a powerful means to eliminate from images the background caused by out-of-focus light and scatter. Confocal techniques can also improve the resolution of a light microscope image beyond what is achievable with widefield fluorescence microscopy. The quality of the images obtained, however, depends on the user's familiarity with the optical and fluorescence concepts that underlie this approach. We describe the core concepts of confocal microscopes and important variables that adversely affect confocal images. We also discuss data-processing methods for confocal microscopy and computational optical sectioning techniques that can perform optical sectioning without a confocal microscope.

One problem with fluorescence microscopy is that, regardless of where the microscope is focused vertically in a specimen, illumination causes the entire specimen thickness to fluoresce. Thus, it is not unusual that in a given two-dimensional (2D) image more than 90% of fluorescence is out-of-focus light that can completely obscure the in-focus detail and greatly reduce the contrast of what remains. For example, a fluorescent cell might be 5 to 15 μm thick, whereas the depth of focus (that is, thickness of the imaging plane) of a high numerical aperture (NA) objective (NA ≥ 1.3) is only about 300 nm or less. Thus the vast majority of the cell volume is out of focus. In addition to light that is out of focus the contrast in fluorescence images is adversely affected by scatter. Scattered light comes from fluorescent emission that may be diffracted, reflected and refracted by the specimen on its way to the objective lens and thus it appears to have been emitted from the last point of scattering and not from the actual location of the fluorophore that emitted it. Because imaging deeper into the specimen increases the chances of scatter, more light will appear to be coming from planes closer to the surface of the specimen than from those deeper inside it, thus producing an image that is more consistent with a specimen preparation in which the concentration of fluorescent dye decreases with specimen depth.

A general approach to improve this problem is to use techniques capable of optical sectioning. Confocal scanning microscopy is presently the most widely used optical sectioning technique for fluorescence imaging, whereas computational optical sectioning techniques allow sectioning using a conventional widefield fluorescence microscope. Multiphoton fluorescence excitation microscopy is an important and very powerful technique for optical sectioning microscopy. This technique is described in detail elsewhere[1], and thus we will not cover it here.

CONFOCAL MICROSCOPY

Optical sectioning acquires images of thin slices of a thick specimen by removing the contribution of out-of-focus light in each image plane. This removal of unwanted light provides greater contrast and permits three-dimensional (3D) reconstructions by computationally combining the image data from a stack of images. Confocal scanning microscopy has an added benefit too: the in-plane or *x-y* resolution of the image can be improved beyond what is possible with conventional widefield fluorescence microscopy. Whereas confocal microscopy can

[1]Molecular, Cell, and Developmental Biology, Oklahoma Medical Research Foundation, Oklahoma City, Oklahoma 73104, USA. [2]Program in Biomedical Engineering, University of Oklahoma, Norman, Oklahoma 73019, USA. [3]Molecular and Cell Biology Department, Harvard University, Cambridge, Massachusetts 02138, USA. Correspondence should be addressed to J.-A.C. (jose-conchello@omrf.ouhsc.edu).

PUBLISHED ONLINE 18 NOVEMBER 2005; DOI:10.1038/NMETH815

10x Genomics EX2046
Bruker v. Harvard
IPR2024-00526

be implemented in many different ways, all of the approaches are based on the same concept. This idea was first described in a patent application by M. Minsky[2] and subsequently described by him in a delightful memoir[3]. Minsky, who is perhaps better known as the founder of the field known as artificial intelligence, as a young man built a confocal microscope to improve reflected-light images of brains in which the Golgi apparatus was stained in hopes of seeing more clearly the connections within a thick tissue block. Whereas his design and theoretical analysis was exactly correct, there was little interest in his idea at the time. He never published a paper using the technique and received no royalties over the 17-year life of the patent.

Subsequent rediscoveries of the confocal idea have led to two rather different implementations, those in which an optical image is directly formed in the retina, film or camera faceplate, and those that must make the images electronically. All confocal techniques, however, share the same fundamental attribute: they are scanning microscopes. 'Scanning' means that the image of each section is built up by adding information from regions that are sampled in sequence. The main drawback of scanning is that image acquisition is not as rapid as wide-field techniques in which the entire image is acquired simultaneously. Thus some implementations aim to speed the process with some potential loss of quality. Other confocal techniques are slower but in principle do not sacrifice any of the potential benefits.

In all confocal microscopes the central concept is to do two things simultaneously (Fig. 1): scan the image by illuminating individual regions in sequence (scanning the illumination) and at the same time mask all but the illuminated regions from providing return light to the detector (scanning the detection). The magnitude of the confocal improvement is inversely related to the size of the region(s) that are sampled at any one moment. To explain why this small scan area is necessary and why the dual scan approach is so effective, we need to dissect the two scanning processes.

CONFOCAL PRINCIPLES

Scanning the illumination and detection

A confocal microscope illuminates one region after another until the whole field of view is sampled. In most confocal microscopes the aim is to illuminate with light that is focused to the very small-

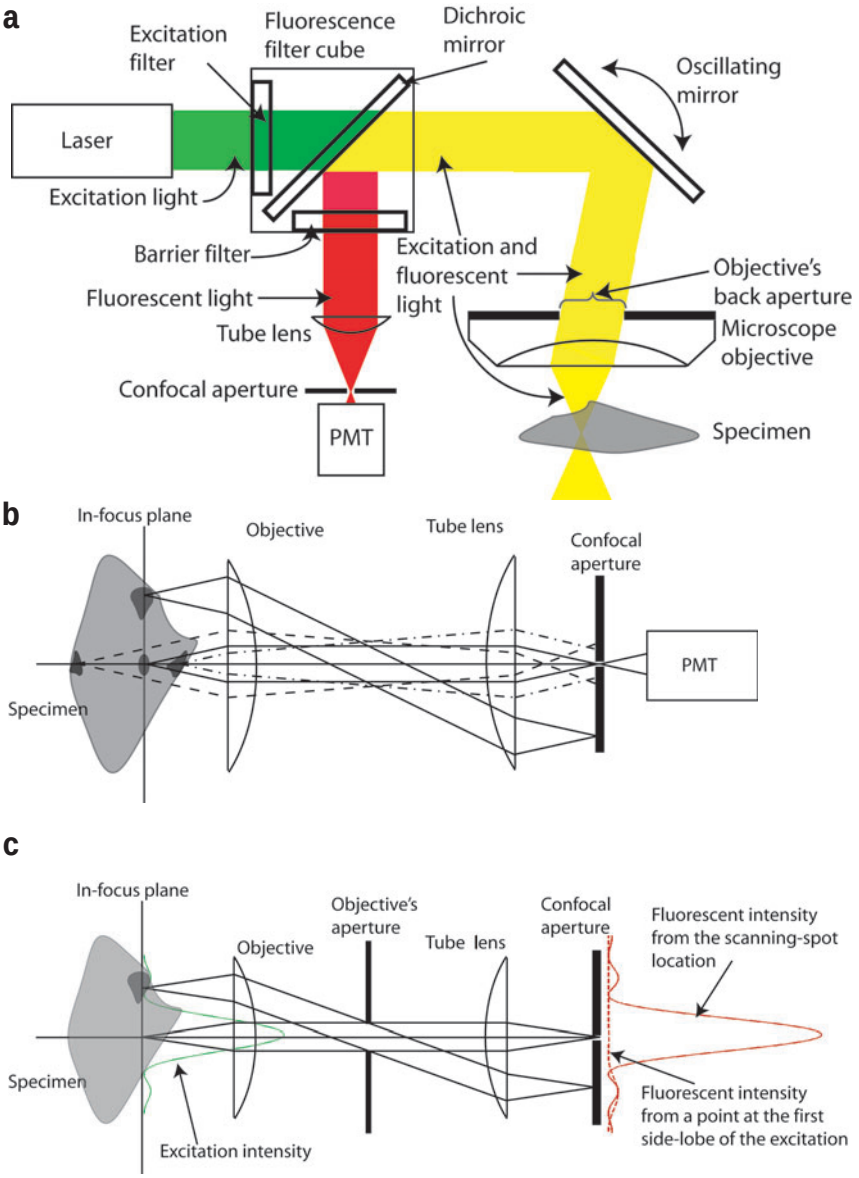

Figure 1 | The confocal principle. (**a**) Layout of the confocal microscope. The excitation light is directed by the scanning mirror and focused into the specimen. The fluorescent emission is separated from the excitation by the dichroic mirror and the barrier filter. Light emitted from the location of the scanning spot goes through the pinhole in front of the detector. (**b**) Path of the fluorescent light with the excitation and scanning not shown. The scanning spot is at the center of the in-focus plane. Light emitted from the in-focus plane (solid lines) is focused into the image plane where the confocal pinhole aperture is located. Light not emitted from the location of the scanning spot focuses on the opaque portions of the pinhole aperture and thus does not reach the PMT detector. Out-of-focus light emitted from points deeper (dashed line) or less deep (dash-dot line) than the in-focus plane come to focus in front or behind the aperture plane, respectively, and thus only a small portion of this light passes through the pinhole aperture. (**c**) The scanning spot (green intensity profile) excites fluorescence. Fluorescent molecules at the location of this spot emit strongly and produce an Airy diffraction pattern at the plane of the confocal pinhole (red solid-line profile), whereas molecules away from this spot weakly fluoresce producing a dimmer Airy diffraction pattern whose peak intensity does not coincide with the pinhole aperture (red dashed-line profile) and, furthermore, their peak intensity does not coincide with the pinhole aperture. As a result, the fluorescence detected from these spots is greatly reduced relative to that coming from the location of the scanning spot.

© 2005 Nature Publishing Group http://www.nature.com/naturemethods

est spot possible in the plane of focus. This diffraction-limited spot of illumination is created by sending a collimated plane wave into the back of the objective where it is transformed into a converging spherical wave by the lens. Thus the full NA of the lens (Fig. 1a) is used to focus the light sharply at a single point at the so-called 'waist' of an hourglass-shaped beam. A laser beam is an ideal light source for this task as it contains all of its energy in a collimated coherent plane wave. In the absence of scattering, the cone of light will focus to its narrowest at the waist of the hourglass-shaped beam (Fig. 2), but because of diffraction, the cone will not evenly illuminate the specimen. This distribution is called the point spread function (PSF) because the image of a small luminous point-object has the exact same pattern. The higher the NA and the shorter the wavelength, the smaller the beam waist will be (diameter = 1.22 λ/ NA, where λ is the wavelength of the excitation light). If the specimen does not absorb light as it passes through the sample, the total amount of illumination is of course the same in all levels of the sample. As the light travels to the waist of the beam, the same amount of light is concentrated into a smaller area, thus the irradiance increases and is highest at the waist. This form of illumination does not selectively illuminate the plane of interest or prevent scattering. Thus, scanning the illumination is insufficient to remove unwanted light, and it is necessary to add some mechanism by which light from out-of-focus sources does not reach the detector. This is achieved by placing a pinhole aperture in front of the detector at a plane that is conjugate to the in-focus plane, such that the illumination spot and the pinhole aperture are simultaneously focused at the same spot (Fig. 1a). Because this microscope requires scanning the illumination spot and having this spot always remain in focus with the pinhole aperture, the instrument is called a confocal scanning microscope (CSM).

Effect on contrast

A measure of the contrast in an image is given by the brightness difference between the signal and the background relative to the background brightness. In widefield fluorescence microscopy the specimen is being illuminated by light converging at every spot in the focal plane simultaneously, and this induces two kinds of background that lower contrast: scatter within the plane of focus and contributions of out-of-focus fluorescence to the in-focus image. Excessive background is the bane of many microscope images. These sources of background are largely removed by confocal imaging.

To get a better idea of how these sources of background arise and why confocal microscopy eliminates them, it is useful to think about what happens with illumination of a single spot with one focused converging spherical wave. In the plane of focus where the light is most intense, some of the exciting light is scattered by particles in the specimen to excite fluorescence out of the region where the focused spot is. This gives a glowing cloud of fluorescence excitation around the waist of the beam. In addition, the return light is scattered on its way out of the tissue, making a fuzzy image of the spot that has the brightest fluorescence. Above and below the plane of focus, the exciting light is less intense but covers a wider area. The net effect is that a uniformly fluorescent sample with negligible absorption and scattering will have the same amount of fluorescence excitation at all depths. Because all but one of these depths is out of focus, the fluorescence from these planes appears as a diffuse background. Scattering in these other planes only makes matters worse. If the sample is thick, the vast majority of the fluorescence signal elicited by illuminating a spot comes from the out-of-focus components.

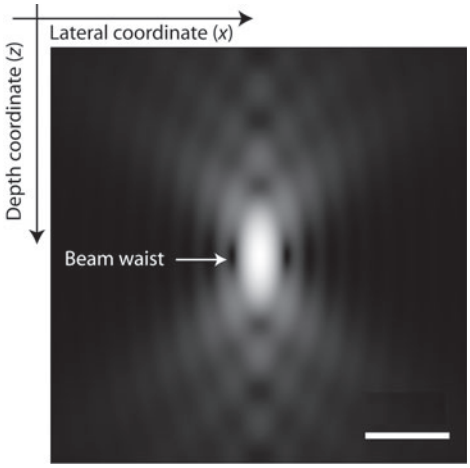

Figure 2 | The PSF. Light distribution near the location of the confocal scanning spot for a 100×, 1.4 NA oil-immersion lens and an excitation wavelength of 530 nm (brightness in log-scale with three decades). Bar, 0.5 μm.

So how can all this background be removed? In the CSM, the pinhole in front of the detector allows the light from the focused spot to reach a detector on the other side of the pinhole (Fig. 1b). At the same time, the pinhole rejects the scattered halo of light around the illuminated spot. It also rejects much, although not all, of the out-of-focus light collected by the objective. This light either is focused before reaching the plane of the pinhole and thus has re-expanded at the pinhole plane, or is on its way to converging to a focused spot but is largely blocked by the pinhole. The pinhole's effectiveness is clearly related to its size, and it might seem that the background would become infinitesimal when the pinhole is very small—even smaller than the projected image of the diffraction-limited spot. The loss of signal, however, eventually outpaces the loss of background, so the optimal pinhole size is between 60% and 80% of the diameter of the diffraction-limited spot[4,5].

The pinhole has no effect at rejecting out of focus background when the sample is illuminated all at once rather than by an hourglass shaped beam because in this case out of focus light getting through the pinhole is no less intense than the in-focus light. The image will be identical to that seen in a widefield fluorescence microscope.

As a result of the selective illumination with an hourglass-shaped beam of only one spot in the plane of focus and an aligned pinhole in a conjugate image plane in the return light path, the light originating from one spot in one plane is selectively detected. This provides excellent contrast because if the exciting light is focused on a spot that does not contain any fluorophores, the detector sees a dark area, and if it contains fluorophores, it sees the light emitted from those fluorophores only. Of course the arrangement just described would only provide the light from one spot. To make an image the scope needs to sample each spot on the specimen plane the same way (the scanning methods for doing this are described below). The accumulated result is a dramatic improvement in contrast and a thin optical section.

Effect on resolution

An important but rarely used property of the CSM is its ability to improve the resolving power of a microscope beyond what is

© 2005 Nature Publishing Group http://www.nature.com/naturemethods

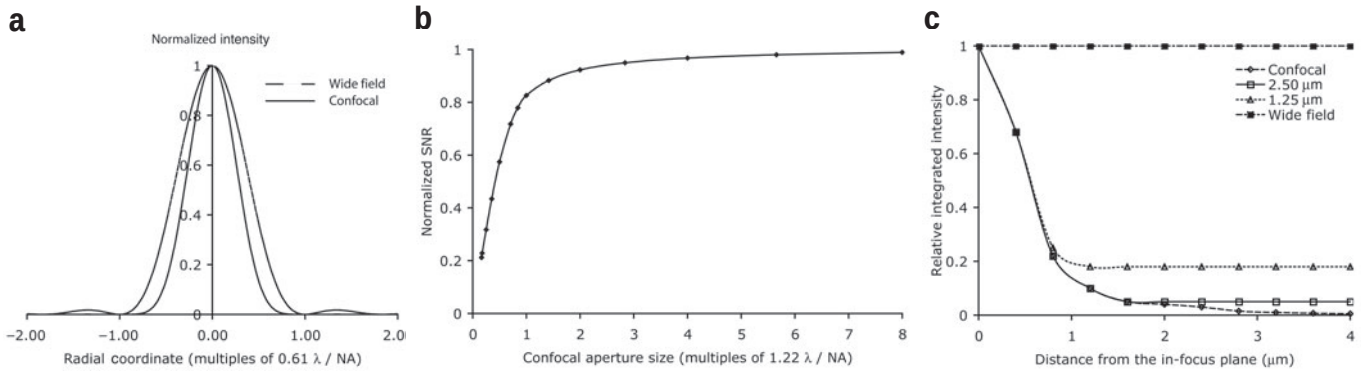

Figure 3 | PSF, SNR and background rejection. (**a**) PSF of the wide-field and confocal microscopes. (**b**) SNR in the confocal microscope with finite aperture normalized such that with a fully open–aperture SNR = 1. (**c**) Background rejection in multiple-aperture confocal scanning microscopy. Graph of overall intensity due to a horizontal thin layer of fluorescence as a function of the distance from focus. For the wide-field microscope the intensity does not change with the distance from the in-focus plane. For the single-aperture confocal microscope it decreases in inverse proportion to the square of the distance from focus. The spinning-disk confocal microscope shows a hybrid behavior. Close to the in-focus plane, the intensity decreases as in the confocal microscope. At more distant planes, the intensity remains constant as in the wide-field microscope. The figure shows this behavior for apertures that are 1.25 µm and 2.5 µm apart (when projected to the specimen). The further apart the apertures are, the stronger the background rejection.

© 2005 Nature Publishing Group http://www.nature.com/naturemethods

achievable with even the highest-NA objectives. This improvement only occurs if the pinhole is stopped down below the size of the central disk of the Airy pattern (< 1.2 λ / NA). To understand why this improvement occurs, consider a confocal beam scanning across a very small fluorescent bead that is itself smaller than the diffraction-limited spot of the scanning beam. The beam itself will project an Airy pattern onto the specimen plane, which in the focal plane will appear as a center bright disc surrounded by concentric rings of progressively lower intensity. As this light approaches the small bead, the first interaction will be between a segment of an outer ring of the illumination spot and the bead. This will give rise to very weak excitation of the bead, whose dim image (also an Airy pattern) will be projected to the site of the pinhole aperture. The pinhole is always aligned with the center of the illumination Airy pattern so only a portion of an outer ring of the image of the bead will be passed through the aperture (Fig. 1c). Given that the bead is being weakly excited and only a small part of the emission is being collected, only an extremely dim part of the fluorescence emitted by the bead will be collected at this point. As the illumination beam moves closer to the bead, the intensity of the excitation of the bead increases and the collection is now from a region of the bead's Airy pattern that contains more emitted light. Finally, when the Airy pattern of the illumination coincides with the bead, the brightest part of the illumination excites the bead, and the brightest part of the emission is collected through the pinhole. The result is that the scanning and pinhole aperture in combination attenuate the Airy pattern of the bead image so that more of the detected intensity is related to the actual position of the bead and not the side rings, which are typically no longer detectable. In addition, the intensity distribution of the central Airy disc is also narrowed for the same reason. In more technical terms, the PSF of the confocal microscope is the product of the PSFs of the objective lens at the excitation and emission wavelengths.

The effect of reducing the rings and also the central disc is that beads that are close together are more easily resolved. In Figure 3a we plotted the intensity profile of the in-focus PSF of a conventional and a confocal scanning microscope. Because the PSF of the confocal microscope is 'pushed down' relative to the PSF of the wide-field-illumination microscope, the PSF is also narrower. This means that the two-point resolution of the CSM is approximately 1.4× better than in a wide-field microscope.

One question that confronts all users of laser scanning confocal microscopes is what is the appropriate size of the pinhole aperture, an easily adjusted parameter in all commercial devices. Based on experimental and theoretical measures of the signal-to-noise ratio (SNR) and optical sectioning (Fig. 3), it is clear that there is a substantial gain in SNR by opening the pinhole aperture to be about the size of the projected image of the diffraction-limited spot (1.22 λ / NA) with little degradation of the depth discrimination[4]. But further increasing the aperture radius marginally increases the SNR but drastically reduces the depth discrimination power of the microscope. The actual optimal size of the pinhole will depend on the magnification of the objective and any relay optics in the path. For example, the optimal pinhole sizes for a 100×, 1.4 NA and a 60×, 1.4 NA objective are in a ratio of 100:60. For the former, the optimal pinhole size is 1.67 times larger than for the latter. In some laser confocal microscopes, the software will give you information about the pinhole diameter in Airy units, with 1 unit being the diameter of the Airy disk. In others, the numbers are measured in millimeters or in arbitrary units, making it a bit more difficult to know exactly what the size is relative to the diameter of the Airy disc requiring you to ask the technical staff of the manufacturer what is the relation for their microscope. This is an important variable and definitely worth knowing.

CONFOCAL SCANNING IMPLEMENTATIONS

Specimen scanning versus illumination scanning

Thus far we have not mentioned how scanning the illumination and collection is achieved. One simple albeit impractical solution is to align the focused light source and the pinhole on the same spot and then raster scan the specimen by moving it with a motorized stage. Whereas such a scheme is used in certain industrial settings, biological samples, especially living ones, will not tolerate the shaking from fast scanning. The main advantage of specimen scanning is that it

avoids off-axis aberrations and thus can be used with a variety of objectives, including those that are not 'plan' and thus suffer from field curvature. In confocal implementations for use in biology, however, the illumination is scanned while the specimen remains still. In illumination scanning, the scanning spot is typically moved in a raster-scan fashion over the specimen. The illumination-scanning mechanism is often away from the stage and thus its vibration, if any, does not affect the location of the specimen relative to the objective. There are several different approaches for illumination scanning. In all implementations, however, if the lens suffers from off-axis aberrations (astigmatism, coma and field curvature), this will degrade the image. Specifically, coma spreads the excitation light away from the location of the aberration-free scanning spot, thus decreasing the amount of fluorescence from this location that reaches the detector. Astigmatism and curvature both move the scanning spot away from the nominal plane of focus, thus exciting light that would otherwise be out of focus.

Laser scanning

The most common method for illumination scanning used by the first commercial CSM designed at the MRC (Biorad MRC 600), and still used today, is based on using two oscillating mirrors to deflect the angle of the light beam going into the specimen (called scanning) and deflecting the angle of emitted light in the return light path (called descanning). One mirror scans the illumination and detection along the 'fast axis' (for example, the horizontal direction), and the other mirror scans the 'slow axis' (for example, the vertical direction). This process continues until an entire 2D image is collected, and it can be repeated at the same focus to generate a time series of images or the focus can be vertically stepped up or down to generate a 3D image stack. The speed of this method is limited by the mechanical characteristics of the fast-axis mirror. It is difficult to drive this mirror to oscillate fast enough to scan at video rates: 30 frames per second, at 512 lines per frame, means that the mirror has to oscillate at $30 \times 512 = 15{,}360$ times per second. It is possible to achieve close to video-rate scanning by using 'resonant' oscillating mirrors (see below). In addition to the mechanical limitation, the time the scanning spot dwells over a pixel is a limitation of the CSM. If a 512×512 image is collected in one second, it means that the spot dwells for $1\ \text{s} / (512 \times 512) \approx 4\ \mu\text{s}$ on each pixel, although it is possible to scan substantially faster ($<<1\ \mu\text{s}$ per pixel). In reference 6, it is calculated that to excite detectable fluorescence in such a short time with a typical sample, it is necessary to deliver about 80 microWatt (μW) of light to each pixel. For brightly fluorescent samples less power can be used, but this still requires laser illumination.

The slow acquisition time derives from the fact that the laser scanning approach builds an image sequentially one pixel at a time. The detector is typically a photomultiplier tube (PMT), which has low noise and a fast response. PMTs are ideal for detecting weak signals, even single photons. Unfortunately PMTs are not very efficient. They detect 10% or less of the fluorescence signal that gets through the pinhole. Thus as scanning speeds increase, the number of detected photons per pixel may drop to such a low number that noise from the PMT will limit the quality of the image. Slow scanning speed is not only an inconvenience, but it also limits the utility of the instrument, especially when rapidly changing signals are being studied. In some cases users do 'line scans' to essentially bypass the slower 2D image for the more rapid speeds possible by using just the fast-scan mirror.

Spinning-disk

One way to decrease the scan time without compromising the SNR is to multiplex: illuminate several pixels simultaneously and collect light from all of them at the same time. One successful method is to use a disc with a series of pinhole apertures. Each aperture illuminates a different spot on the specimen and the emitted fluorescence is then focused onto another pinhole aperture on the disk[7,8] or through the same one[9,10]. In the most common form, the fluorescent image of the illuminated spots coincide with the location of the pinholes on the disk, thus the pinholes serve both to focus spots of light on the specimen and also as the confocal pinholes. The light that passes through the apertures is then imaged on a detector. In this case the detector is either the retina or a camera, typically a charge-coupled device (CCD) or intensified CCD camera. The arrangement of the pinhole apertures over the disk is such that as the disk rotates, the illumination spots scan the entire field of view of the microscope.

A notable advantage of the spinning-disk CSM is that, because many spots can be illuminated simultaneously (typically hundreds or more over the field of view) and rapid rotation of the disc illuminates the same spot several times within a frame time (for example, within the 33 ms exposure required for video rate), the total dwell time can be much larger than for the CSM with a single pinhole aperture. This increase in dwell time allows for much faster frame rates. A variation of this spinning-disk CSM that affords potentially faster frame rates has slit apertures on the disk, but its principle is otherwise similar, that is, rotation of the disk makes the slits illuminate the entire specimen (a simple and inexpensive plan for a such a microscope can be found in[11,12]).

One disadvantage of the spinning-disk CSM as described is its rather inefficient use of the excitation light. For example, if the pinholes occupy only 1% of the disc area 99% of the illumination of the disc is wasted. A new design for the spinning-disk CSM ('Yokogawa' design) was introduced in which another disk with an array of microlenses is placed on top of the pinholes on the illumination side of the disk. These lenses are illuminated by a collimated laser beam, which the lenses focus into the pinholes, thus greatly increasing the illumination efficiency of the spinning-disk CSM to about 60% or more. Because it is difficult and expensive to build a microlens array that does not suffer from chromatic aberration, two disks need to be used, one for the apertures and the other for the microlenses. A fluorescence filter cube is placed between the two disks so the microlenses are not in the fluorescent return-light path[13,14].

The spinning-disk CSM presents a trade-off between resolution and SNR in terms of the aperture size. In commercially available spinning-disk CSMs, the aperture size is fixed during manufacturing and cannot be adjusted. The size, type and spacing of the aperture on the disc control the background rejection capabilities of the microscope.

In CSMs, the brightness of the out-of-focus excitation decreases with the square of the distance from the in-focus plane. This is because, as already mentioned, the excitation light has an hourglass shape with the waist at the in-focus plane and with the total amount of light the same in each plane. The area over which it is distributed is the area of the circle resulting from the intersection of the cone with the out-of-focus plane. Since this area increases with the square of the out-of-focus distance, the excitation that a pixel receives decreases with the square of this distance. This inverse square law holds as long as out-of-focus structures are illuminated by a single aperture on the disk, but in the spinning-disk CSM, many apertures are used

© 2005 Nature Publishing Group http://www.nature.com/naturemethods

Table 1 | Useful spectral lines for lasers available for confocal microscopy

Laser	Useful lines (nm)
Argon ion (Ar)	257, 488, 514
Kripton ion (Kr)	531, 568, 647
Ar-Kr	488, 568, 647
Helium-neon (He-Ne)	543, 594, 612, 633
Helium-nadmium (He-Cd)	442
Zinc-Selenium (Zn-Se) diode	430
Neodymium–yttrium aluminum garnet (Nd-YAG)	532, 355, 266
Neodymium–yttrium lithium fluoride (Nd-YLF)	527, 349, 262

to illuminate the specimen. Each of these apertures produces a two cone–shaped illumination about the specimen. Close to the in-focus plane, the cones from different apertures in the disk are distant from each other so that out-of-focus material is illuminated by at most one cone. As the distance from the in-focus plane increases, however, the cones from apertures adjacent in the spinning disc come closer to each other until at some distance (which depends on the NA of the lens and the distance between the apertures[15]), the cones from different apertures cross and more than one cone (and thus by more than one aperture) excite fluorescence. It can be shown that from that distance on, the excitation intensity does not decrease with the out-of-focus distance but remains constant, although at a much lower level than in the wide-field illumination microscope[15].

Figure 3c compares the background discrimination capabilities of the spinning-disk CSM against those of the wide-field and the single-pinhole aperture confocal microscopes. The closer the apertures are, the larger the constant background intensity and the closer to the in-focus plane it remains constant.

Line scanning

Another method to increase the dwell time without decreasing the frame rate is to illuminate an entire line of the specimen simultaneously and focus the fluorescence into a linear CCD array (that is, a row of CCD wells). The use of line illumination obviates the need for scanning the fast axis using an oscillating mirror. Currently, there is one commercial line-scan CSM, the Zeiss LSM 5 Live. This CSM achieves video frame rates by exciting with a line illumination and using a slit confocal aperture. In addition, the microscope can have more than one fluorescent channel and thus can simultaneously detect more than one fluorophore. A slit-confocal-aperture microscope, however, does not afford the resolution improvement of a spot scanning system.

Other scanning approaches

Over the years there have been ingenious attempts to increase the speed of the fast axis scan such as a rotating mirrored polygon[16], or a series of holographic or curved mirrors mounted on a rotating disk, such that each mirror illuminates a different pixel in the specimen[17]. Another method is to drive the fast-axis mirror at its resonance oscillating frequency. In this approach, the fast-axis oscillating mirror and the galvanometer that controls its position are designed such that their resonant frequency is fast enough for video rate scanning, then the electronics drive the mirror at that frequency. One notable custom-built version of this microscope has been described[18]. In a conventional CSM, the raster scan is such that the time between adjacent pixels along the fast scan axis is the same across the scanned field. With the resonant-mirror approach, however this no longer holds. This is because when the mirror is driven at its resonant frequency, the position of the scanning spot across the scan field changes with time according to a sinusoid. This has the potential problem of non-uniform bleaching.

Lasers

Confocal microscopes come with a wide range of options concerning lasers. A purchaser needs to decide which laser lines will be needed to excite the fluorophores in use. The recent advent of solid state lasers adds more choices. The most common workhorse is the multiline argon-ion laser which can emit from the UV (230 nm) to the green (514 nm) with useable power at 257, 477 and 514 nm. Helium-neon (He-Ne) lasers are inexpensive and although they are single-line, they provide useful coverage from the green to the red with useful lines at 534, 567, 594 and 612 nm. Although they have less power than most lasers, power is rarely the limitation that prevents good confocal imaging. Krypton-ion lasers also provide a good selection of lines from the green to the red. When combined with argon; (Ar-Kr laser), it provides lines from the blue to the red. Users who need blue light for CFP use either a helium-cadmium (He-Cd) at 440 nm, a finicky laser, or solid state lines of the zinc-selenium (Zn-Se) diode laser. Users interested in DAPI or some calcium-indicator dyes require UV excitation. At the moment these wavelengths are possible mainly from large argon lasers that sometimes need water cooling. Recently, diode-pumped or lamp-pumped semiconductor lasers that emit in the infrared, such as the neodymium-yttrium aluminum garnet (Nd-YAG) and neodymium-yttrium lithium fluoride (Nd-YLF), have been combined with nonlinear crystals that generate second-, third- or fourth- harmonics. This combination gives lines in the green, UV and deep UV[19]. The lines for different lasers are summarized in Table 1.

POTENTIAL PROBLEMS

Bleaching

The use of the CSM brings with it several potential problems that do not apply to the wide-field microscope. Foremost among them is the increased risk of bleaching. The probability that a molecule bleaches depends on its exposure to the excitation light. This is the product of the irradiance a molecule receives and the time it receives it. Thus, a molecule that receives irradiance I_1 of duration t_1 is as likely to bleach as one that receives twice the irradiance ($2I_1$) for half the time ($t_1/2$). In a CSM, the excitation light is spread over an area that increases with the square of the out-of-focus distance. Consequently, the irradiance decreases in proportion to the square of the distance. Conversely, the time a pixel is exposed is proportional to the area of the excitation and thus to the square of the out-of-focus distance. Therefore, the product of the time an out-of-focus molecule is exposed and the irradiance it receives is almost the same at every depth if the effects of scattering and absorption are negligible. As a result, in-focus and out-of-focus molecules bleach at almost the same rate. With the high irradiance and low per-frame rates typical of the CSM, photobleaching is a serious drawback for many specimens.

When the scanning mechanism uses oscillating mirrors, bleaching occurs not only while the microscope is collecting data, but also during the retrace when the scanning spot is moving back to the beginning of the next image line. During the retrace time, the laser is exciting fluorescence that is not being collected but nonetheless is

© 2005 Nature Publishing Group http://www.nature.com/naturemethods

bleaching the fluorophore. Placement of a shutter that closes at the end of each line and opens at the beginning of the next, adds to the already long frame scan time of the CSM. Another approach, used in the Zeiss 510 CSM, is to use an acousto-optic tunable filter (AOTF) to prevent fluorescence excitation during the retrace. Because the AOTF has no moving parts, it can be tuned very quickly to block or to pass the excitation light and thus does not increase the scan time.

SNR, NA and magnification

The processes of photon absorption, emission and detection are random and thus the numbers of photons measured from two pixels with equal amounts of fluorophore are similar but not equal. This random variation gives the image a grainy appearance that is stronger for lower image irradiance. Ideally, one would attempt to maximize the number of photons per pixel to increase the SNR. In practice, however, there are limitations and trade-offs to balance (Box 1). The characteristics of the CSM that have the largest effects on image SNR are the size of the pinhole and the NA of the objective.

The light-gathering efficiency of a microscope is proportional to the square of the objective's NA. When also used for illumination, as in confocal scanning microscopy, the overall sensitivity of the CSM is proportional to $(NA)^4$ and is unaffected by magnification power because in the CSM the pinhole aperture size can be adjusted according to the NA and magnification of the objective to obtain the same resolution and SNR with both objectives. For example, the PSF in front of the pinhole for a 100×, 1.4 NA objective is 100 / 60 = 1.67 times larger than the PSF of a 60×, 1.4 NA objective at the same wavelength. Thus, opening the pinhole aperture by a factor of 1.67 will achieve the same resolution and SNR with both objectives. In addition, the CSM has the advantage of an electronic zoom that allows a user to obtain additional (even if empty) magnification by scanning a smaller area with the same number of pixels. Although the electronic zoom does not degrade the SNR, it causes faster photobleaching because the closer the pixels are in the specimen, the longer the excitation dwells over neighboring pixels and thus bleaches them faster.

BOX 1 TROUBLESHOOTING AND CAVEATS

LOW SIGNAL

Effective signal strength measured by the SNR is impacted by many different factors as discussed below.

NA of the objective. The NA of the objective is one of the most critical variables that impacts signal quality in a CSM. Because resolution is determined by the NA and the pinhole size, but is independent of magnification, the best image is obtained by using an objective with a higher NA rather than a higher magnification.

Pinhole size. Reducing the pinhole size rejects more background light and thus increases the depth discrimination. But it also produces a grainy appearance in the image owing to the reduction in the signal compared to random variations recorded by the detector. The optimal pinhole size is between 60% and 80% of the diffraction-limited spot. In practice, larger pinholes must often be used when imaging dim samples or fluorophores that bleach easily. Alternatively, increasing the pinhole beyond ($1.22\,\lambda$ / NA when projected to the specimen) reduces effective imaging depth. With newer bleach-resistant fluorescent quantum dots, however, it may be easier to image with smaller pinhole diameters. Pinholes smaller than 60% of the diffraction limited spot, however, actually worsen the grainy appearance of the image.

PMT gain. Increasing the gain on the PMT will increase the signal but also results in higher shot noise. Such a trade-off may be necessary if bleaching is a problem. This increase in signal and noise is different than the increase that results from 'brightness' control in that the latter increases signal and noise by the same amount and thus has no effect on the grainy appearance of the recorded image.

Laser power. Increasing the laser power is a simple way of increasing the apparent signal but greatly increases the risk of sample bleaching and, more importantly, fluorescence saturation as well as other deleterious effects, so all other optimizations should be attempted first.

Decreasing graininess. The grainy appearance can also be ameliorated by increasing the signal by a larger factor than the random variations that cause the grainy appearance. This can be accomplished by increasing the dwell time at the risk of increased bleaching. It is also possible to increase the scanning speed and reduce the laser power while using filtering methods to combine data from multiple scans.

Fluorophore concentration. The fluorescent emission intensity is proportional to the concentration of fluorescent dye, but there are practical limitations to this concentration. A very high concentration could have toxic effects on the organism under study, interfere with the process being observed, or leave a large amount nonspecific fluorescence. To avoid these pitfalls, the concentration of fluorescent dye is usually kept low with a resulting low fluorescence intensity that brings a low SNR. Quantum dots and other new fluorophores with improved characteristics can help reduce these problems.

SLOW IMAGING

For users of fluorescence widefield microscopes in which video-rate or faster imaging is relatively straightforward, the slow rate of data flow in laser scanning confocal microscopes can be frustrating. Thus, for moving the stage and finding objects of interest, many users still resort to direct viewing of the widefield fluorescence image by eye and then initiating a scan. Most modern laser scanners, however, have a 'focus' mode with scans of 5 or more frames per second. Although these images are noisy and severely undersample the data, they may serve to speed the process of finding a particular spot to image. When data itself must be sampled quickly, 'line scans' are an option.

BLEEDTHROUGH

It is becoming increasingly common to simultaneously use two or more fluorescent dyes for imaging different properties or structures of the specimen. If more than one dye is present, however, a channel designed for a particular dye will collect fluorescence from other dyes whose excitation and fluorescence spectra overlap with the dye of interest. When this is not taken into account and compensated for, the recorded images for a given dye are artifactual because of contributions from other dyes. The linear unmixing methods described in the text can effectively separate the different dyes.

© 2005 Nature Publishing Group http://www.nature.com/naturemethods

Conversely, in the wide-field microscope, the objective magnification has a strong effect on the image SNR. Given two objectives with the same NA and using the same camera, the objective with the larger magnification spreads the light over a larger area in proportion to the square of the magnification.

Too much scatter (deep imaging)

When a CSM is used to image detail within a relatively thick layer of tissue, the excitation and the emission photons must travel through the tissue where molecular interactions will change their direction. As a result, the excitation light is spread over a volume much larger than the diffraction-limited spot and thus the excitation is weaker over a larger volume. The fluorescence emitted from a molecule within this volume can be scattered on its way to the objective so that it no longer seems to come from the scanning spot. Thus, out-of-focus light might appear to come from the location of the scanning spot whereas in-focus light is rejected because it is scattered by out-of-focus tissue. The resulting image has two major degradations, namely, it is severely blurred and has a very low SNR. For deep imaging in tissue, two-photon fluorescence microscopy may be more suitable[1].

DATA PROCESSING

Averaging approaches

Despite the marked improvement in contrast owing to rejection of out-of-focus light, images from CSMs have low SNR because of the small number of photons that can be excited from each pixel in the short time the pixel is under the scanning spot. This problem is obvious in the graininess of many confocal images. Some users attempt to correct this problem by increasing the laser power during the scan, but this is generally a mistake. The laser intensity possible in most commercial laser scanning confocals far exceeds that necessary to saturate the fluorophore in the focal plane. In other words, the fluorescent molecules at the waist of the hourglass-shaped beam are cycling between excited state and ground state as fast as they can, and greater illumination irradiance provides no additional fluorescence. On the other hand, increased illumination will cause increasing amounts of out-of-focus light to percolate through the pinhole, causing the image to loose resolution in all dimensions. If one keeps the laser power low (that is, <~1.5 mW for a scanning spot 0.5 μm across[20]) one can still improve the SNR by collecting several images of the same plane and averaging or adding them. The two most widely used methods are a simple average and the Kalman filter, which is an auto-regressive moving-average filter (for a detailed description of the Kalman filter see[21,22]). Each pixel of the final image is obtained from measurements of the same pixel at different times. As these averaging approaches operate in time, not space, they have little or no effect on the resolution (strictly speaking, there is a degradation in resolution because the scanning mechanism may not place the scanning spot precisely enough during repeated scans).

In the simple average filter all the 2D images are simply averaged. This increases the SNR in direct proportion to the square root of the number of frames that are averaged. That is, averaging four frames doubles the SNR, whereas averaging 16 increases the SNR by a factor of $(16)^{1/2} = 4$. The Kalman filter is a more elaborate statistical filter that uses auto-regression of prior measurements to predict the present measurement and then corrects the estimate with a moving average as soon as the present measurement is available. The strongest advantage of the Kalman filter over simple filtering is that it requires very few frames (typically less then 5) to reach a steady value for each pixel, whereas the simple average requires more frames. The disadvantage of the Kalman filter is that it assumes that noise is additive. Although not strictly correct, this assumption has little effect on the results when the number of photons per pixel is above ~20. In cases with a lower number of photons, simple averaging might be a better choice of method.

Another approach to noise reduction is to increase the dwell time by slowing the scan speed. Most commercial laser scanners allow the user to adjust the scan time over a wide range. This approach has one drawback: as a population of fluorophores are excited they tend to progressively partition into the long-lived triplet state where they are no longer able to fluoresce and are subject to bleaching. Thus, with a long duration exposure of each pixel, the laser excitation will first initiate good fluorescence but within several hundred nanoseconds the same laser intensity will become less effective[20]. In summary, fast scanning with low power and averaging is probably the best way to obtain a good image, although the ability of the scanning mirrors to accurately go to exactly the same position may tend to blur these images a bit. Some trial and error is required to find the best noise reduction method for a particular device.

Linear unmixing

The large cadre of fluorescent probes available at different wavelengths provides both unprecedented opportunities for multispectral imaging and a problem: crosstalk between different fluorescent signals. The most straightforward approach to disambiguating fluorescence signals is to sequentially record images at the emission wavelengths of the different fluorescent dyes. Sequential scanning gives excellent separation of fluorophore images because both the excitation and emission can be altered (as with standard filter cubes). The problem with sequential imaging is that if one wishes to take a stack of images the time of imaging increases in proportion to the number of images. A stack of 100 images with three fluorophore sequential imaging in which each image is averaged three times to remove noise will take ~15 min. A second problem with sequential imaging is that it is sometimes unable to remove crosstalk because the dyes' absorption and emission spectra overlap too much. This is a considerable problem with fluorescent proteins that typically have wide emission and absorbance spectra[23], though newer variants are helping to reduce this problem[24]. CSMs offer the possibility of simultaneous scanning because the emitted light can routinely be beam-split to different detectors to collect different emission wavelengths. The wavelengths can be separated by color filters (for example, dichroic or interference filters) or spatially by a prism that takes advantage of dispersion to produce a rainbow-colored pattern. This dispersion is used by Leica spectral confocal microscopes, to bring different colors of light to different detectors.

One serious drawback of trying to image more than one fluorescent dye at a time, however, is that the overlap of excitation and emission spectra make it difficult or even impossible to find an emission wavelength that detects one fluorophore and none of another. A solution is to record what is sometimes called a λ scan, which is a fluorescence excitation spectrum of all the dyes while exciting with one or more wavelengths. Unlike a typical spectrum done at one point, this scan is done spatially on a whole image plane. The number of spectral points in the scan must equal or exceed the number of dyes one is trying to separate. Taking images at several wavelengths takes time. In the Zeiss version of this approach (Meta) a prism is used to

© 2005 Nature Publishing Group http://www.nature.com/naturemethods

obtain the spectral images simultaneously. In the Olympus configuration the λ scan is done sequentially. In both cases, however, the narrowness of the spectral bands reduces the SNR, requiring averaging and more time. Conversely, the λ scan does provide access to the full fluorescence emission of a fluorophore and using the emission spectra of each different fluorophore to identify the contribution of each provides a means of eliminating crosstalk[24–28].

To see how this method works, assume that a specimen is stained with three different fluorescent dyes (Fig. 4a). Cyan fluorescent protein (CFP; triangles) has a peak emission at 477 nm, fluorescein isothiocyanate (FITC; squares), at 535 nm, and tetramethyl rhodamine isothiocyanate (TRITC; circles), at 575 nm. The rectangles in Figure 4a represent the ideal response of barrier filters commonly used for the three dyes. It is clear that there is substantial overlap of the three spectra and that none of the filters completely rejects fluorescence from another dye. The superposition of images collected with the three filters is shown in Figure 4b. We have circled and labeled three spots that have different concentrations of the three fluorescent dyes. Spot 1 has 10% CFP, 30% FITC and 60% TRITC. Spot 2 has 10% CFP, 60% FITC and 30% TRITC. Finally, Spot 3 has 70% CFP, and 15% each FITC and TRITC. The individual images collected with the three filters show that the three labeled spots appear in more than one image not only because of the mixture of dyes but also because of the overlap of the three spectra (Fig. 4c–e). Emission curves show the λ scan at each of the three fluorescent spots and the vertical bars show the readings obtained using the barrier filters for each of the three dyes assuming that each filter collects all the fluorescence within its passband (Fig. 4f–h). Using these profiles and the spectra in Figure 4a, it is possible to write a set of linear equations that relate the relative concentrations of the three dyes to the amount of light measured by each detector. Using the measured intensities from the detectors the linear equations can be solved to obtain the amount of each of the fluorescent dyes at each of the spots. This is called linear unmixing, and it is not restricted to unmixing three dyes. By using at least as many channels and filters as there are fluorescent dyes in the sample, it is possible to unmix more dyes, and additional channels will reduce the effects of noise.

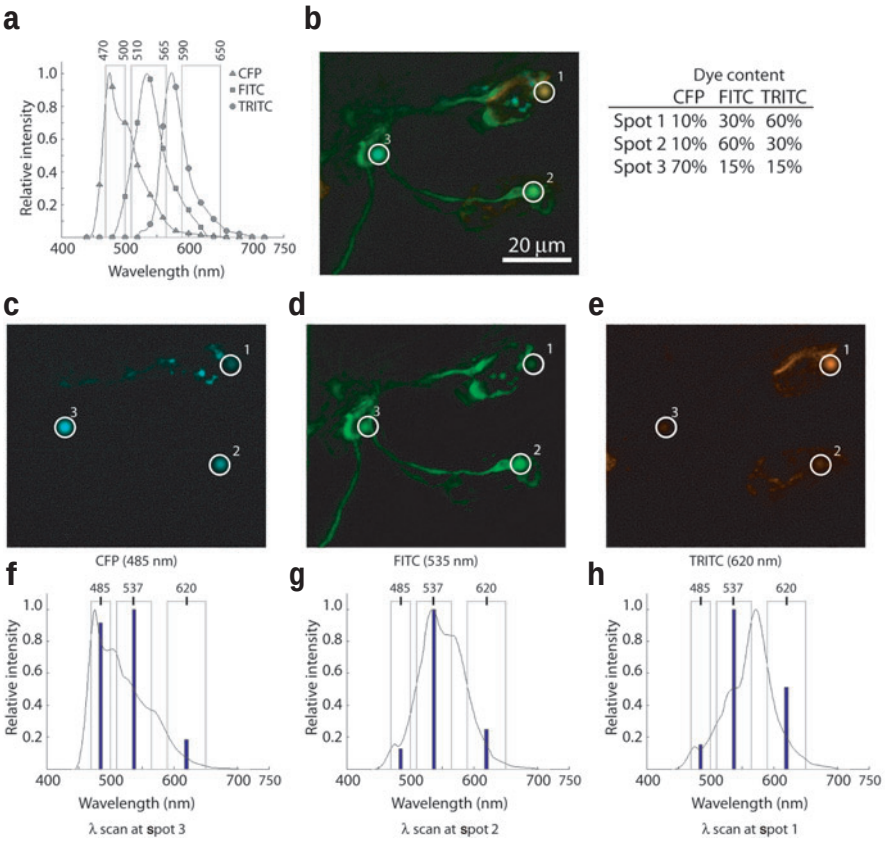

Figure 4 | Linear unmixing. (**a**) Emission spectra for CFP, FITC and TRITC. The rectangles represent the ideal response of barrier filters commonly used for the three dyes. The numbers on top of the rectangles are the cut-off wavelengths for each of the filters. (**b**) Color composite made with the images recorded at the peaks of the three dyes. The three spots marked with circles have known mixtures of the three dyes. (**c**–**e**) Images obtained with each of the three barrier filters. (**f**–**h**) λ scans at each of the three spots circled in **c**–**e** collected with ideal narrow-band barrier filters. As in **a**, the rectangles are ideal responses of the three barrier filters commonly used for the three dyes. The vertical bars indicate the response collected by the detector with each of the three filters at each of the three spots (the bars are placed at the mean wavelength of each filter; this wavelength is indicated at the top of each rectangle).

OTHER OPTICAL SECTIONING TECHNIQUES

Deconvolution (computational optical microscopy)

A method that has steadily gained acceptance as an alternative as well as a complement to confocal scanning and two-photon fluorescence excitation microscopy is computational optical sectioning microscopy (COSM), also known as deconvolution microscopy and sometimes as 'digital confocal' (although the latter is a misnomer because in COSM with a widefield microscope, the specimen is under Köhler illumination and thus excitation is maximally out of focus at the specimen, whereas the term confocal means excitation and detection are in focus at the same point). In COSM, as with a CSM, a 3D image is collected as a series of 2D images (or optical slices), each with the microscope focused at a different plane through the specimen. If a wide-field microscope is used, each of the 2D images has the in-focus information plus substantial contributions from out-of-focus material. In COSM, a computational method derived from information about the process of image formation and recording is used to remove the out-of-focus light from each optical slice. Several methods have been derived for COSM whose differences stem from the different mathematical models used for the process of image formation and recording. Because a very accurate model for the process of image formation and recording would be mathematically and computationally intractable, different models rely on different simplifying assumptions. Better models of the process of image formation and recording lead to better results, usually at the expense of higher computational cost. The earliest models were heavily simplified and led to methods with very low computational demands. As comput-

© 2005 Nature Publishing Group http://www.nature.com/naturemethods

ing power increased, it allowed the use of methods based on more exact formulations of the imaging process, and algorithm developers tapped into the increased computer power to derive methods based on more precise models. Here we will briefly touch on the results and limitations of some methods (Fig. 5). For a more thorough review see reference 29.

Nearest neighbors deconvolution. One of the first COSM methods, called nearest neighbors subtraction (NNS), is based on a simple model of image formation, namely that out-of-focus light from a given optical slice is relevant only in the two adjacent slices. To undo this degradation, the method blurs the adjacent slices with a 2D PSF calculated for a miss-focus distance equal to the distance between adjacent optical slices and subtracts them from the optical slice of interest to remove the out-of-focus light. The result can be filtered with a Wiener-type filter to remove some of the in-focus blur. This process is repeated for all the optical slices. Although the method is based on a very simplified model, it applies when the fluorescent light rapidly decreases away from the focus, as for small puncta, thin filaments, or a combination of them. For example, in a single optical slice of fluorescently labeled actin filaments extracted from a 3D image stack (Fig. 5a) the NNS method effectively removes the out-of-focus blur (Fig. 5b). For specimens in which the fluorescence covers larger areas (for example, cell membranes) or volumes (for example, neuromuscular junctions), the simple model does not apply and a different approach is necessary.

Frequency-based deconvolution. One such different approach is based on how the microscope images periodic structures. Given a periodic structure, such as a diffraction grating, the contrast in the image greatly depends on the frequency of the structure (measured, for example, in cycles per μm). For small frequencies, the image shows very good contrast, but as the frequency of the grating is increased (the distance between adjacent stripes reduced), the contrast is reduced until it vanishes completely when the frequency of the grid reaches 2 NA / λ. Frequencies higher than this cut-off frequency are not passed by the microscope to the image. The way the microscope images periodic structures is mathematically described by the optical transfer function (OTF). This is the Fourier transform of the PSF of the microscope. Any image can be analyzed into a series of periodic structures of different frequencies, amplitudes and phases that, when superimposed, give rise to the image. These series of structures are called the frequency components of the image. It is computationally straightforward to obtain the frequency components of an image by using a Fourier transform.

Because the frequency components of the image are the frequency components of the specimen multiplied by the OTF, the frequency components of the specimen can be obtained by dividing the image frequency components by the OTF. This simple operation, however, is not possible because the OTF is zero for all frequencies above the cut-off frequency. The two most widely-used approaches to avoid this division by zero are the Moore-Penrose pseudo-inverse (MPPI; Fig. 5c)[30] and the Wiener or, more properly, Wiener-Helstrom filter (WHF, Fig. 5d). Each of these methods introduces a small arbitrary correction factor ε, thus avoiding the division by zero, but use different methods of doing so. For a thorough description see reference 31. The choice of ε controls the tradeoff between the resolution and the amount of noise in the resulting specimen estimate. Small ε results in finer resolution but more noise. The MPPI and WHF operate on the whole 3D stack, not on each optical slice as the NNS, and thus they can remove out-of-focus light from more distant planes. An optical slice from a 3D image of fluorescently labeled membranes of *Hystoplasma capsulatum* is shown in Figure 5e. The NNS not only does not remove the out-of-focus light inside the membrane, but results in a grainy appearance that gives the impression of a specimen made of small puncta (Fig. 5f). Both the MPPI and the WHF, however, remove the out-of-focus light and do not 'break' the cell membrane into a series of spots (Fig. 5g,h).

© 2005 Nature Publishing Group http://www.nature.com/naturemethods

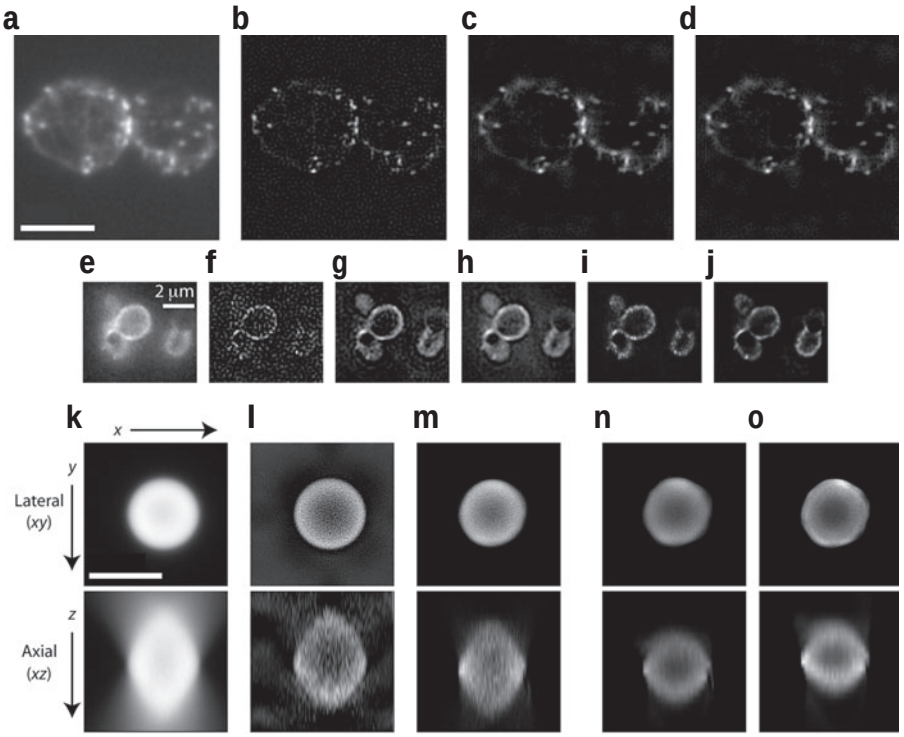

Figure 5 | Deconvolution results. (**a**–**d**) A specimen consisting mostly of puncta and thin filaments (images courtesy of T. Karpova, National Cancer Institute). The original image slice (**a**) and deconvolutions obtained using NNS (**b**), MPPI (**c**) and WHF (**d**) methods. Bar, 5 μm. (**e**–**j**) *H. capsulatum* with the cell membrane fluorescently labeled (images courtesy of W. Goldman, Washington University School of Medicine). The original image slice (**e**) and deconvolutions obtained using NNS (**f**), MPPI (**g**) and WHF (**h**), JvC (**i**) and the expectation-maximization maximum-likelihood (**j**) methods. Bar, 2 μm. (**k**–**o**) Sections through the center of a 3D image stack of a 10-μm diameter polystyrene microsphere (images courtesy of J.G. McNally, National Cancer Institute). Top, lateral section; Bottom, axial section. The original image slice (**k**) and deconvolutions obtained using a MPPI (**l**), JvC (500 iterations, smoothing every 10 iterations; **m**), constraint maximum-likelihood expectation maximization (3,000 iterations; **n**) and gradient-based method (100 iterations; **o**). Bar, 10 μm.

© 2005 Nature Publishing Group http://www.nature.com/naturemethods

Constraint deconvolution. One serious drawback of the methods described above is that they cannot estimate frequency components of the specimen at frequencies that are not passed by the objective. These frequencies, however, are often necessary for the correct estimation of the specimen. For example, image sections through the center of a 3D image stack of a 10-µm-diameter polystyrene microsphere with a thick superficial fluorescent layer 1 to 2 µm thick are shown in Figure 5i. This image has two problems. (i) There is no fluorescent dye in the core of the microsphere but the image shows a bright core and (ii) although the specimen is a sphere, the *xz* section has a diamond shape in addition to dimmer 'butterfly wings'. We have demonstrated that the diamond shape results from the lack of important frequency components[32]. Because the image lacks frequency components, the MPPI can not recover the spherical shape of the specimen and only partially removes the 'butterfly wings' from the image (Fig. 5j). The results from the WHF (not shown) are similar. Because these frequency components are not in the image, it is necessary to derive algorithms that use information about the specimen known *a priori*. This information might be the fact that fluorescence is neither negative nor infinite or that the specimen has a finite size. Prior knowledge about the specimen is used to enforce constraints that the specimen estimate must satisfy. Incorporating these constraints into the algorithm usually leads to iterative methods that perform several operations over and over until certain criteria are satisfied.

The most widely used methods for constraint deconvolution are the Jansson-van Cittert (JvC) method of repeated convolution[33] as modified in reference 34 and commercially distributed by Applied Precision; the constrained least squares method developed by Carrington[35,36] and distributed by Scanalitics; and the maximum-likelihood image estimation independently developed by Holmes[37,38] and by Conchello[4,39,40] from the expectation maximization formalism[41]. The Holmes method is commercially distributed by AutoQuant Imaging and the Conchello method is freely available online (http://www.omrfcosm.omrf.org). Although the JvC method does correctly find the dark core of the microsphere and removes the 'butterfly wings' it still shows the diamond shape in the axial section (Fig. 5m). The expectation maximization–maximum likelihood method recovers the spherical shape of the specimen albeit at the expense of a large number of iterations (Fig. 5n). The maximum-likelihood estimation method, however, can be improved by using a different method than expectation maximization to find the maximum of the likelihood function. In fact, by using a gradient-based algorithm we found a substantial increase in speed with little or no degradation in performance (Fig. 5o)[42].

New wide-field techniques

In recent years, new methods for optical sectioning microscopy have been developed for wide-field illumination, which do not use uniform illumination. Instead, these methods give some spatial structure to the illumination. The most notable ones are aperture-correlation microscopy[43–46] and sine-modulated illumination microscopy. The former method, however, required a large number of images to be collected at each focal plane and thus found little application. The latter, which is more often called structured illumination microscopy (SIM), is a simpler and more powerful method for optical sectioning microscopy[47–55]. In SIM, a sinusoidal illumination pattern is focused by the objective into the in-focus plane of the specimen and an image I_1 is collected. The pattern is then shifted laterally by a third of the cycle of the pattern, and a second image I_2 is collected. The illumination pattern is shifted a second time a third of its cycle and a third image is recorded. Each of these images contains both in-focus and out-of-focus information. The in-focus information, however, is modulated by the sinusoidal illumination pattern, whereas the out-of-focus information is much less affected by the structure of the illumination. There are two simple ways to remove the sinusoidal illumination pattern from the images. One is by simply averaging of the three images. The result, however, is the image that would have been obtained with a conventional wide-field microscope. That is, it contains the out-of-focus light. The other is to calculate

$$I_p = \frac{\sqrt{2}}{3}\sqrt{(I_1 - I_2)^2 + (I_1 - I_3)^2 + (I_3 - I_2)^2}\ .$$

The pairwise subtraction of images removes the parts that are common to the images in the pair. This is mostly out-of-focus light that was not affected by the structure of the illumination. Thus, the resulting image contains little out-of-focus light. In fact the depth resolution possible with the SIM is similar to that achievable with the CSM. To our knowledge, there is currently only one commercial version of the SIM, namely the Zeiss Apotome (Karl Zeiss). Because the price of the Apotome is much less than that of a laser CSM, the SIM is sometimes called a 'poor-man's confocal microscope'.

CONCLUSIONS

Optical sectioning microscopy is a powerful tool for biological investigation, and confocal microscopy is often the method of choice. As explained above, CSMs have the capability to record 3D images that are not affected by out-of-focus light, thus increasing the contrast and resolution of the recorded image. In addition, the wide selection of available fluorescent probes, lasers and filters makes the CSM a powerful tool for multispectral imaging when aided by linear unmixing. In addition to the CSM, the 'digital confocal microscope' and the 'poor-man's confocal microscope' provide alternative methods for 3D microscopy that have image collection times much shorter than those typical of the CSM. The interested user is encouraged to read available literature [56–68].

COMPETING INTERESTS STATEMENT
The authors declare that they have no competing financial interests.

Published online at http://www.nature.com/naturemethods/
Reprints and permissions information is available online at http://npg.nature.com/reprintsandpermissions/

1. Helmchen, F. & Denk, W. Deep tissue two-photon microscopy. *Nat. Methods* **2**, 932–940 (2005).
2. Minsky, M. (US patent 3013467, 1961).
3. Minsky, M. Memoir on inventing the confocal scanning microscope. *Scanning* **10**, 128–139 (1988).
4. Conchello, J-A., Kim, J.J. & Hansen, E.W. Enhanced 3D reconstruction from confocal scanning microscope images. II: depth discrimination vs. signal-to-noise ratio in partially confocal images. *Appl. Opt.* **33**, 3740–3750 (1994).
5. Sandison, D.R., Piston, D., Williams, R.M. & Webb, W.W. Quantitative comparison of background rejection, signal-to-nose ratio, and resolution in confocal and full-field laser scanning microscopes. *Appl. Opt.* **34**, 3576–3588 (1995).
6. Tsien, R.Y. & Waggoner, A. Fluorophores for confocal microscopy. In *Handbook of biological confocal microscopy* (ed. Pawley, J.B.) 267–279 (Plenum Press, New York, 1995).
7. Petràn, M., Hardvsky, M., Egger, M.D. & Galambos, R. Tandem scanning reflected-light microscope. *J. Opt. Soc. Am.* **58**, 661–664 (1968).
8. Petràn, M., Boyde, A. & Hardvsky, M. Direct view confocal microscopy. In *Confocal Microscopy* (ed. Wilson, T.) 245–284 (Academic Press, New York, 1990).

9. Kino, G.S. & Xiao, G.Q. Real-time scanning microscopes. In *Confocal Microscopy* (ed. Wilson, T.) 361–388 (Academic Press, London, 1990).
10. Lichtman, J.W. Confocal microscopy. *Sci. Am.* **271**, 30–35 (1994).
11. Lichtman, J.W. High-resolution imaging of synaptic structure with a simple confocal microscope. *New Biol.* **1**, 75–82 (1989).
12. Lichtman, J.W. & Sunderland, W.J. (Washington Univeristy; US patent 4884880, 1990).
13. Inoué, S. & Inoué, T. Direct-view high-speed confocal scanner: The CSU-10. In *Cell biological applications of confocal microscopy* (ed. Matsumoto, B.) 88–128 (Academic Press, New York, 2002).
14. Tanaami, T. *et al.* High-speed 1-frame/ms scanning confocal microscope with a microlens and a Nipkow disk. *Appl. Opt.* **41**, 4704–4708 (2002).
15. Conchello, J-A. & Lichtman, J.W. Theoretical analysis of a rotating-disk partially confocal scanning microscope. *Appl. Opt.* **33**, 585–596 (1994).
16. Stutz, G.E. Laser scanning system design. *Photonics Spectra* **24**, 113–116 (1990).
17. Tsien, R.Y. & Bacskai, B.J. Video-rate confocal microscopy. In *Handbook of biological confocal microscopy* (ed. Pawley, J.B.) 459–478 (Plenum Press, New York, 1995).
18. Callamaras, N. & Parker, I. Construction of a confocal microscope for real-time x-y and x-z imaging. *Cell Calcium* **26**, 271–279 (1999).
19. Gratton, E. & vande Ven, M. J. Laser sources for confocal microscopy. In *Handbook of biological confocal microscopy* (ed. Pawley, J.B.) 69–97 (Plenum Press, New York, 1995).
20. Sandison, D.R., Williams, R.M., Wells, K.S., Stricker, J. & Webb, W.W. Quantitative fluorescence confocal laser scanning microscopy (CLSM). In *Handbook of biological confocal microscopy* (ed. Pawley, J.B.) 39–53 (Plenum Press, New York, 1995).
21. Srinath, M.D. & Rajasekaran, P.K. *Statistical Signal Processing with Applications* (John Willey and Sons, New York, 1979).
22. Kay, S.M. Fundamentals of statistical signal processing (Prentice Hall, 1993).
23. Lichtman, J. & Conchello, J.-A. Fluorescence microscopy. *Nat. Methods* **2**, 910–919 (2005).
24. Shaner, N.C., Steinbach, P.A. & Tsien, R.Y. A guide to choosing fluorescent proteins. *Nat. Methods* **2**, 905–909 (2005).
25. Zimmermann, T. Spectral imaging and linear unmixing in light microscopy. In *Microscopy techniques advances in biochemical engineering/biotechnology* **95**, 245–265 (2005).
26. Zimmermann, T., Rietdorf, J. & Pepperkok, R. Spectral imaging and its applications in live cell microscopy. *FEBS Lett.* **546**, 87–92 (2003).
27. Zimmermann, T., Rietdorf, J., Girod, A., Georget, V. & Pepperkok, R. Spectral imaging and linear un-mixing enables improved FRET efficiency with a novel GFP2-YFP FRET pair. *FEBS Lett.* **531**, 245–249 (2002).
28. Hiraoka, Y., Shimi, T. & Haraguchi, T. Multispectral imaging fluorescence microscopy for living cells. *Cell Struct. Funct.* **27**, 367–374 (2002).
29. Conchello, J.-A. An overview of three-dimensional and four-dimensional microscopy by computational deconvolution. In *Cell Imaging-Methods Express* (ed. Stevens, D.) 181–204 (2005).
30. Preza, C., Miller, M.I. & Thomas, L.J. Jt. & McNally, J. G. Regularized linear method for reconstruction of three-dimensional microscopic objects from optical sections. *J. Opt. Soc. Am. A* **9**, 219–228 (1992).
31. Frieden, B.R. *Probability, statistical optics, and data testing.* 206–210 (Springer-Verlag, Berlin, Germany, 1982).
32. McNally, J.G., Preza, C., Conchello, J-A. & Thomas, L.J., Jr. Artifacts in computational optical sectioning microscopy. *J. Opt. Soc. Am. A* **11**, 1056–1067 (1994).
33. Frieden, B.R. Image enhancement and restoration. In *Picture processing and image filtering* (ed. Huang, T.S.) 179–248 (Springer-Verlag, New York, 1975).
34. Agard, D.A. Optical sectioning microscopy. *Annu. Rev. Biophys. Bioeng.* **13**, 191–219 (1984).
35. Carrington, W.A. Image restoration in 3D microscopy with limited data in *Bioimaging and two-dimensional spectroscopy* (ed. Smith, L.C.) 72–83 (SPIE Press, Bellingham, Washington, 1990).
36. Carrington, W.A. & Fogarty, K.E. (US patent 5047968, 1991).
37. Holmes, T.J. Maximum-likelihood image restoration adapted for noncoherent optical imaging. *J. Opt. Soc. Am. A* **5**, 666–673 (1988).
38. Holmes, T.J. & Liu, Y-H. Richardson-Lucy/maximum likelihood image restoration algorithm for fluorescence microscopy: further testing. *Appl. Opt.* **28**, 4930–4938 (1989).
39. Conchello, J-A. Super-resolution and convergence properties of the expectation maximization for maximum-likelihood deconvolution of incoherent images. *J. Opt. Soc. Am. A* **15**, 2609–2619 (1998).
40. Conchello, J-A. & Hansen, E.W. Enhanced 3D reconstruction from confocal scanning microscope images I: Deterministic and maximum likelihood reconstructions. *Appl. Opt.* **29**, 3795–3804 (1990).
41. Dempster, A. P., Laird, N. M. & Rubin, D. B. Maximum likelihood from incomplete data via the EM algorithm. *J. R. Stat. Soc. B* **39** 1–38 (1977).
42. Markham, J. & Conchello, J-A. Fast maximum-likelihood image restoration algorithms for three-dimensional fluorescence microscopy. *J. Opt. Soc. Am. A* **18**, 1062–1071 (2001).
43. Hanley, Q.S., Verveer, P.J. & Jovin, T.M. Optical sectioning fluorescence spectroscopy in a progammagle array microscope. *Appl. Spectrosc.* **52**, 783–789 (1998).
44. Verveer, P.J., Hanley, Q.S., Verbeek, P.W., van Vliet, L.J. & Jovin, T.M. Theory of confocal fluorescence imaging in the programmable array microscope (PAM). *J. Microsc.* **189**, 192–198 (1998).
45. Wilson, T., Juskaitis, R., Neil, M.A.A. & Kozubek, M. Confocal microscopy by aperture correlation. *Opt. Lett.* **21**, 1879–1881 (1996).
46. Dixon, T. Microscopy - Random mask brightness image. *Nature* **383**, 760–761 (1996).
47. Neil, M.A.A., Juškaitis, R. & Wilson, T. Method for obtaining sectioning by using structured light in a conventional microscope. *Opt. Lett.* **25**, 1361–1363 (1997).
48. Wilson, T., Neil, M.A.A. & Juškaitis, R. Optically Sectioned images in wide-field fluorescence microscopy. In *Three-dimensional and multidimensional microscopy: Image Acquisition and Processing V* (eds. Cogswell, C.J., Conchello, J.-A., Lerner, J.M., Lu, T. & Wilson, T.) 4–6 (SPIE Press, Bellingham, Washington, 1998).
49. Gustafsson, M.G.L., Agard, D.A. & Sedat, J.W. Doubling the lateral resolution of wide-field fluorescence microscopy using structured illumination. In *Three-dimensional and multidimensional microscopy: image acquisition and processing VII* (eds. Conchello, J.-A., Cogswell, C.J. & Wilson, T.) 141–150 (SPIE Press, Belingham, WA, 2000).
50. Gustafsson, M.G.L., Agard, D.A. & Sedat, J.W. Surpasing the lateral resolution by a factor of two using structured illumination microscopy. *J. Microsc.* **198**, 82–87 (2000).
51. Neil, M.A.A., Juškaitis, R. & Wilson, T. Real time 3D fluorescence microscopy by two beam interferece illumination. *Opt. Commun.* **153**, 1–4 (1998).
52. Neil, M.A.A., Juškaitis, R. & Wilson, T. A light efficient optically sectioning microscope. *J. Microsc.* **189**, 114–117 (1998).
53. Wilson, T., Neil, M.A.A. & Juškaitis, R. Real-time three-dimensional imaging of macroscopic structures. *J. Microsc.* **191**, 116–118 (1998).
54. Gustafsson, M.G.L. Extended resolution fluorescence microscopy. *Curr. Opin. Struct. Biol.* **9**, 627–634 (1999).
55. Fedosseev, R., Belyaev, Y., Frohn, J. & Stemmer, A. Structured light illumination for extended resolution in fluorescence microscopy. *Opt. Lasers Eng.* **43**, 403–314 (2005).
56. Conn, P.M. (ed.) *Confocal Microscopy* (Academic Press, New York, 1999).
57. Diaspro, A. (ed.). Confocal and two-photon microscopy: Foundations, applications and advances. (John Wiley and Sons, New York, 2001).
58. Inoué, S. & Spring, K.R. *Video Microscopy. The Fundamentals* (Plenum Press, New York, 1997).
59. Matsumoto, B. (ed.). *Cell biological applications of confocal microscopy* (Academic Press, New York, 2003).
60. Murphy, D.B. Fundamentals of light microscopy and electronic imaging (Wiley-Liss, New York, 2001).
61. Pawley, J.B. (ed.). *Handbook of biological confocal microscopy* (Plenum Press, New York, 1995).
62. Paddock, S. (ed.). *Confocal Microscopy* (Oxford University Press, Oxford, 2001).
63. Periasamy, A. (ed.). *Methods in Cellular Imaging* (Oxford University Press, Oxford, 2001).
64. Sheppard, C.J.R. & Shotton, D.M. *Confocal Laser Scanning Microscopy* (BIOS Scientific Publisers, Oxford, 1997).
65. Stevens, J.K., Mills, L.R. & Trogadis, J.E. *Three-dimensinoal confocal microscopy: Volume investigation of biological systems* (Academic Press, New York, 1994).
66. Toomre, D. & Manstein, D.J. Lighting up the cell surface with evanescent wave microscopy. *Trends Cell Biol.* **11**, 298–303 (2001).
67. Tsien, R.Y. Imagining imaging's future. *Nat. Rev. Mol. Cell. Biol.* **4** (Suppl.), SS16–SS21 (2003).
68. Yuste, R., Lanni, F. & Konnerth, A. (eds.) *Imaging neurons: A laboratory manual* (Cold Spring Harbor Laboratory Press, Cold Spring Harbor, 2000).

© 2005 Nature Publishing Group http://www.nature.com/naturemethods